Journal of Archaeological Science: Reports 49 (2023) 104013

Contents lists available at ScienceDirect

Journal of Archaeological Science: Reports

journal homepage: www.elsevier.com/locate/jasrep

Reconstruction of archaeological contexts through the integrated use of airborne LiDAR and geophysical survey: The case study of San Pietro Infine (Caserta, southern Italy)

Rosa Di Maio [a,*], Antonio Emolo [b], Alessia Frisetti [c], Nicodemo Abate [d], Mauro La Manna [a], Ivano Pierri [a], Rosanna Salone [a], Stefania Tarantino [b,e]

[a] *Dipartimento di Scienze della Terra, dell'Ambiente e delle Risorse, Università degli Studi di Napoli Federico II, Complesso Universitario di Monte S. Angelo, via Cintia, 21, 80126 Napoli, Italy*

[b] *Dipartimento di Fisica "Ettore Pancini", Università degli Studi di Napoli Federico II, Complesso Universitario di Monte S. Angelo, via Cintia, 21, 80126 Napoli, Italy*

[c] *Dipartimento di Scienze Umanistiche, Università degli Studi Suor Orsola Benincasa, corso Vittorio Emanuele, 292, 80132 Napoli, Italy*

[d] *Consiglio Nazionale delle Ricerche – Istituto di Scienze per il Patrimonio Culturale, C.da S. Loja, 85050 Tito Scalo, Potenza, Italy*

[e] *Istituto Nazionale di Geofisica e Vulcanologia, viale Francesco Crispi 43/45, 67100 L'Aquila, Italy*

ARTICLE INFO

Keywords:
Geophysical prospecting
LiDAR remote sensing
Landscape archaeology
Ad Flexum Roman settlement
Southern Italy

ABSTRACT

San Pietro Infine (Caserta, southern Italy) is an archaeological area of significant historical interest as it is in the vicinity of the Roman site of *Ad Flexum*. Based on historical sources, the site would correspond to the junction of a road axis that, during the Roman colonization (3rd century BCE), was crossed by the *Via Latina*. At the intersection of these two roads, which coexisted for a time, a post station was built, most likely later replaced by an early medieval village near the religious building of S. Pietro, of which only the apse portion is preserved. However, the archaeological evidence is too scarce to allow a reliable historical reconstruction of the site and to direct any excavation work. In this paper, we present the integration of LiDAR and geophysical surveys with the aim of advancing the archaeological interpretation of the San Pietro Infine site over the-state-of-the-art while providing a cutting-edge example in archaeological investigation. In particular, LiDAR data analysis was addressed to recognize and characterize topographic micro-reliefs presumably correlated to buried archaeological structures, while subsurface geophysical prospecting, consisting of magnetic and electromagnetic surveys, was aimed at defining their possible location and extent in depth, due to the expected contrasts in the magnetic and electric properties between the targets (e.g., limestone materials, paving roads) and the host geological setting (mainly marshy deposits). The integrated study allowed us to identify a structure whose characteristics (i.e., location, shape and nature) could well match the hypothesized *Ad Flexum* junction. In addition, LiDAR micro-reliefs and geophysical anomalies individuate structures that, by location and extent, suggest the presence of a village developed around the religious building of San Pietro.

1. Introduction

Santa Maria del Piano (Fig. 1a), located south-west of the modern village of San Pietro Infine (Caserta, southern Italy), is an area of relevant archaeological interest because it includes the Roman site of *Ad Flexum* (Fig. 1b), whose location has long been a subject of debate (Mommsen, 1883; Carettoni, 1940). However, it was not until the 1980s that the correct setting of the site could be defined, thanks to some archaeological traces found following the widening of a gravel road and the excavation of a segment of the Venafro-Rocca D'Evandro railway line (Fig. 1a). The importance of the area is proved since pre-roman times because it was the junction of a road axis controlled by the fortified settlements of Sant'Eustachio and Colle Marena-Falascosa at the foothills of Mt. Sambucaro (Fig. 1a; Zambardi, 2007a, b). During the Roman colonization occurring in the 3rd century BCE, the pre-existing road axis was crossed by the *Via Latina* (Fig. 1b), as demonstrated by

* Corresponding author.
E-mail addresses: rosa.dimaio@unina.it (R. Di Maio), antonio.emolo@unina.it (A. Emolo), alessia.frisetti@docenti.unisob.na.it (A. Frisetti), nicodemo.abate@imaa.cnr.it (N. Abate), mauro.lamanna@unina.it (M. La Manna), ivano.pierri@unina.it (I. Pierri), rosanna.salone@unina.it (R. Salone), stefania.tarantino@unina.it (S. Tarantino).

https://doi.org/10.1016/j.jasrep.2023.104013
Received 11 January 2023; Received in revised form 7 April 2023; Accepted 12 April 2023
Available online 21 April 2023

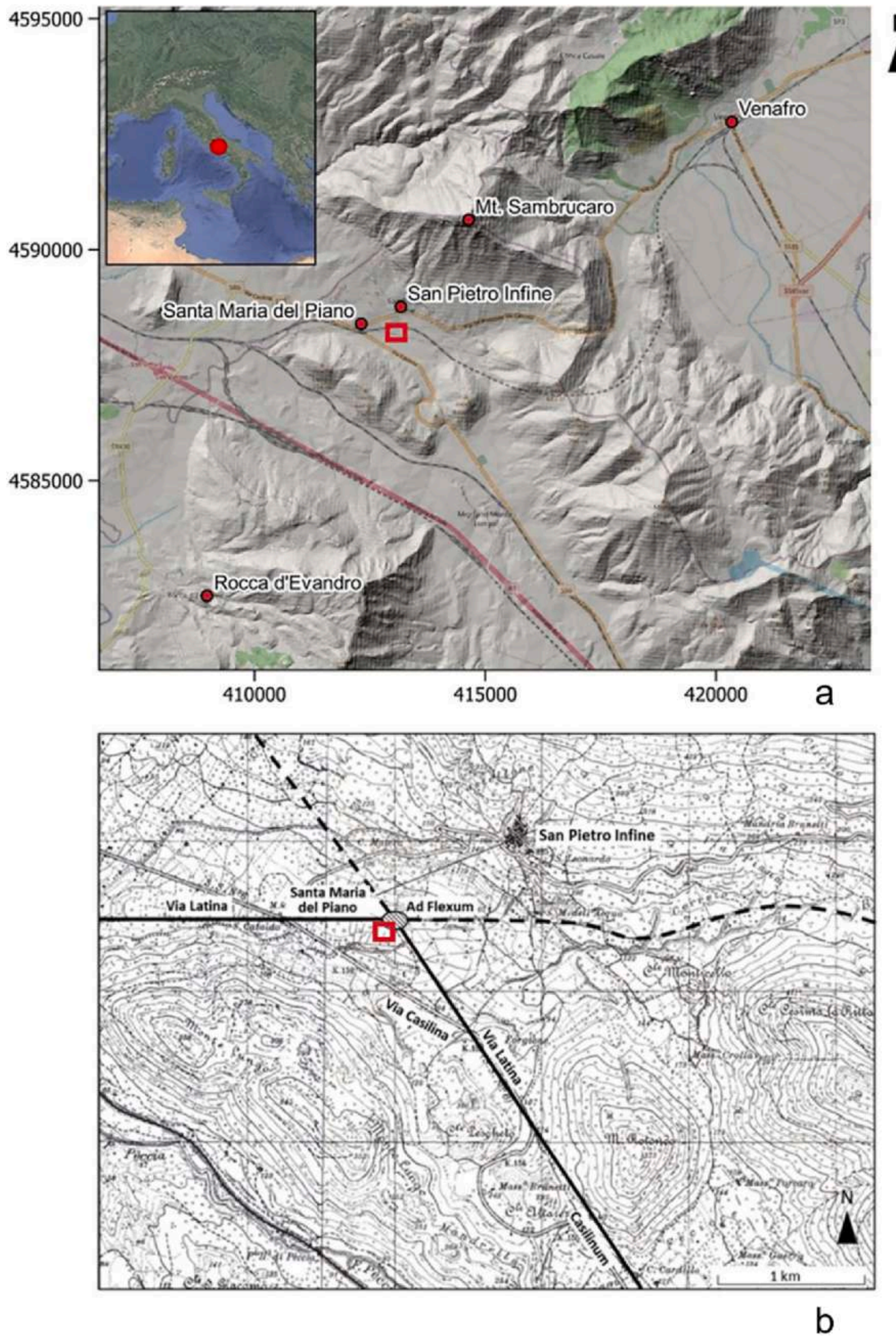

Fig. 1. a) Location of San Pietro Infine (Caserta, southern Italy). b) Framing of the *Ad Flexum* site (from Zambardi, 2007b, modified) on the topographic map extracted from the IGMI (Italian Military Geographic Institute) base cartography at scale 1:25000 - sheet 161 – III-N.O. Venafro. The red rectangle indicates the geophysical survey area. (For interpretation of the references to colour in this figure legend, the reader is referred to the web version of this article.)

the paving stones found near Santa Maria del Piano (Zambardi, 2007b). In the area characterized by the intersection of these two roads, which coexisted for a time, a *mansio* (post station) was built, most likely later replaced by a *pagus* (village). The toponym *Ad Flexum*, transcribed in the *Tabula Peutengeriana* (Calzolari, 2003), probably originates from the paved segment of the road found near the *mansio*. This segment, in fact, flexes toward the Roman settlement of *Casilinum* (Fig. 1b) (Caiazza, 1995; Merola, 2007; Zambardi, 2007a, b). The historical importance of this area is evidenced by the human presence also in the Middle Ages, when the Roman post station was replaced by a rural village born around the church of S. Pietro, of which only the apse portion is preserved. Indeed, the church belonged to the Benedictine Abbey of Montecassino. There are several examples of rural villages that grew up around small monastic churches in the Middle Ages (Frisetti, 2019; Marazzi, 2011; Marazzi, 2016). These villages were usually inhabited by small groups of peasants who worked the land for the religious communities and attended mass in the church of S. Pietro. We can therefore assume the presence of various small rural houses, built with poor and easily degradable materials (e.g., wood, straw, clay), a small cemetery near the church, all surrounded by vegetable gardens and cultivated fields. Between the 8th and 10th centuries, through these rural churches, monastic communities ensured the exploitation of previously uncultivated lands and the loyalty of local families. However, the archaeological evidence is too scarce to enable a reliable historical reconstruction of the site as well as to address any excavation work. Therefore, an integrated interpretation of the results from LiDAR (ALS, Airborne Laser Scanning) surveys and subsurface geophysics, combined with information from the archaeological findings, was used to get a consistent picture of the ancient site of San Pietro Infine that could guide future archaeological research. The goal of our study is both to advance the archaeological interpretation of the San Pietro Infine site above the state-of-the-art, and to integrate information from different approaches into a coherent archaeological interpretation, in order to provide a leading-edge example in this research field. Specifically, ALS data analysis was devoted to the identification and characterization of topographic micro-reliefs presumably related to buried archaeological structures, while geophysical prospecting was aimed at defining their possible location, shape and extension in depth. In particular, for finer and more reliable characterization of the entire system under investigation, i.e. anthropogenic remains and hosting geological setting, a multimethodological geophysical approach was used. Based on the geological background of the test site, which consists mainly of marshy material due periodical runoffs of the river shaft flowing south of the study area, the following geophysical methods were used: magnetic, frequency-domain electromagnetic and ground penetrating radar. In fact, these techniques are able to detect the expected contrasts in the physical properties between the geological background and the survey targets, mainly consisting of limestone/brick masonry and paving roads. The multimethodological geophysical prospecting was performed in an area that surrounds *Il Torrione* (Id 1 in Fig. 2), an outcropping structure

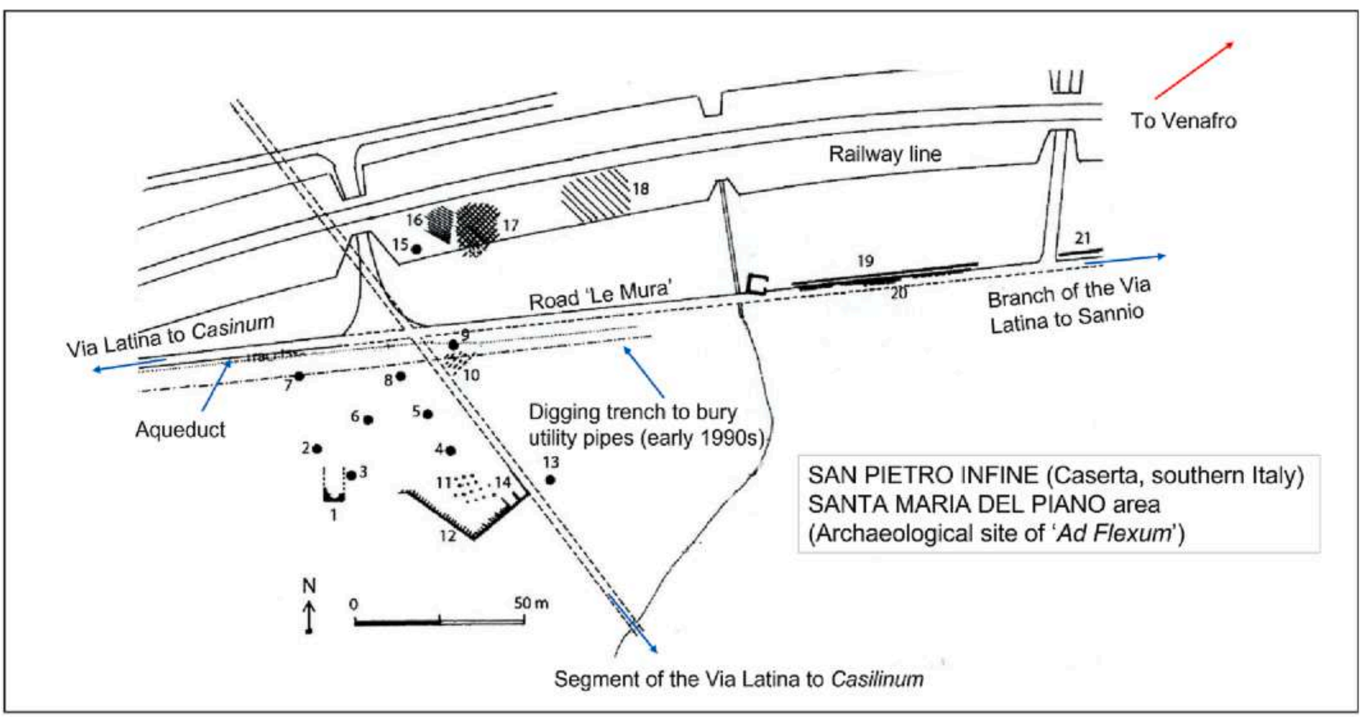

1. The so-called '*Il Torrione*', with the apse of the S. Maria del Piano Church
2. Marble head probably attributed to Emperor Adrian
3. Roman marble basin with zoomorphic motifs
4. Limestone block with groove
5. Limestone fragment of Roman inscription
6. Fragment of base of Roman statue (right foot)
7. Segment of a vaulted sewerage
8. Big limestone blocks and paving stones
9. Archaeological stratigraphy
10. Several fragments of tiles, mortar and bones
11. Several small blocks of "*opus reticulatum*"
12. Retaining wall with stones and mortar
13. Cylindrical limestone block
14. Masonry structures perpendicular to the wall (no. 12)
15. Big limestone block with moldings (probably the base of a statue)
16. Archaeological finds
17. Mosaic pavement and archaeological finds (arrowheads, coins, human bones, glass, tiles, pottery, boar's teeth)
18. Masonry structures
19. A segment of the Via Latina, a sidewalk and a wall in "*opus incertum*"
20. Paving stones of the Via Latina
21. A segment of the Via Latina, a sidewalk and a wall in "*opus incertum*"

Fig. 2. Plan of San Pietro Infine site (Caserta, southern Italy) showing the various archaeological findings (from Zambardi, 2009a, modified).

referable to an apse belonging to a layered religious complex (Zambardi, 2007a), which is considered by archaeologists as relevant for the reconstruction of the ancient Roman settlement. Moreover, to verify the hypotheses based on the archaeogeophysical interpretation, a forward modeling of the acquired magnetic data was performed to define the location of the supposed buried structures and to estimate their magnetic susceptibility contrast with the geological background.

2. The archaeological site of San Pietro Infine

2.1. Geological setting

The San Pietro Infine archaeological area is located in the northern sector of the Campania region (southern Italy, see inset in Fig. 1a), along the boundary with both Lazio and Molise regions, not far from the Roccamonfina extinct volcano. It lies in a narrow plain bordered to the north and south by mountain ridges crossed by the *Via Casilina* (Fig. 1b), an ancient Roman road. The reliefs are mainly formed by Mesozoic limestones and dolomitic limestones, and the morphotectonic setting results in a graben-like structure formed because of high-angle faults that affected the limestone belt. The depressed areas at the foothills are filled by alluvial and volcanoclastic deposits, whose emplacement is linked to the occurrence of several streams that drain the run-off of waters from the carbonate massifs. The investigated archaeological site was buried by reworked deposits of the Roccamonfina volcano mainly made up of variably sized tuff clasts embedded in an altered sand-silty argillified matrix.

2.2. Historical and archaeological context

The archaeological records at the ancient site of San Pietro Infine are rather fragmentary because they come from surveys and emergency excavations carried out in the 1980s. However, these data show that the site of *Ad Flexum* was in the area of Santa Maria del Piano (Fig. 1). First, evidence of the importance of the site can be gleaned from an honorary epigraph from the Republican period that documents considerable building development of the settlement (Giannetti, 1973). On the other hand, tracks of *Via Latina* are suggested by some paving stones found during the widening of a gravel road in *Le Mura* site (Fig. 2) at a depth of about 0.70 m from the ground level. The portions of the paved road brought to light (Id 19, 20 and 21 in Fig. 2) have an E-W direction, and are, therefore, assumed to belong to a branch of the *Via Latina* that led to the Roman town of Venafro (Zambardi, 2009a; Fig. 2). The presence of the Roman road in this sector of the archaeological site is also confirmed by the finding of a milestone (*miliarium*) dated to the last 3rd-4th century CE, and traces of some building structures (i.e. an *opus spicatum* floor and plastered walls) found at a depth of approximately 0.80 m from the ground surface about 100 m west of the paved road (Zambardi, 2007a). Other remains, notably a mosaic floor and some building structures (Id 17 and 18 in Fig. 2, respectively), were found during the construction of the Venafro-Rocca d'Evandro railway line (Zambardi, 2009a). Furthermore, along the branch of the *Via Latina* that presumably led to the *Via Casilina*, a portion of a retaining wall with NW-SE direction was recovered (Id 12 in Fig. 2). It bends eastward after 50 m and engages perpendicularly with some structures that outcropped about 0.80 m above the ground level, which are no longer visible due to later levelling by the landowner (Zambardi, 2009a). The use of the area in medieval times is evidenced by the remains, called *Il Torrione* (Id 1 in Fig. 2), of the church of Santa Maria del Piano; they may correspond to the apse of the church, which probably overlapped with the older church of *Sancti Petri in Flea*. The latter is mentioned in written sources dating back to the end of the first millennium AD, where it is inferred that the site was known as *oppidum Sancti Petri in Flea*, a toponym derived from the name *Ad Flexum*. Some authors (e.g., Merola, 2007) attribute this *oppidum* to a fortified settlement located in the valley near the church of San Pietro/Santa Maria.

3. Materials and methods

3.1. Airborne LiDAR survey

During the past decades, studies based on the use of airborne LiDAR (Light Detection And Ranging) data in archaeology have increased exponentially. This technology, to date used by both airplane and drone, is probably the best performing currently among the Remote Sensing techniques applied to archaeology for the identification of archaeological sites and topographical micro-reliefs created by anthropogenic actions/structures both under canopy (Briese and Pfeifer, 2001; Masini et al., 2011; Lambers, 2018; Luo et al., 2019; Adamopoulos and Rinaudo, 2020; Cohen et al., 2020). In the modern literature, there are many studies related to discoveries and studies of archaeological contexts under vegetation, such as those conducted by, for instance, Khan et al. (2017) in the evolution of the ancient landscape covered by the Amazon rainforest, Chase et al. (2011) for the study of ancient Maya civilizations, Evans et al. (2013) in ancient Angkor Wat in Cambodia, and Masini et al. (2018) in medieval Italian contexts. At the same time, an increase in LiDAR-based work in archaeology has been matched by an increase in methodological studies with the development of *ad-hoc* solutions for this field, such as the open source tools developed by Kokalj et al. (2019), Lozić and Štular (2021), and Štular et al. (2021a), or solutions based on derived DTM (Digital Terrain Model) data, illumination engineering, and artificial intelligence that have proven useful for the identification of archaeological remains (Crutchley, 2006; Corns and Shaw, 2009; Banaszek, 2013; Doneus, 2013; Evans et al., 2013; Costa-García et al., 2016; Horňák and Zachar, 2017; Kokalj and Hesse, 2017; Davis et al., 2019; Štular and Lozić, 2020; Guyot et al., 2021; Richards-Rissetto et al., 2021; Štular et al., 2021b; Štular et al., 2023) as well as for the identification of cultural heritage hazardous phenomena such as looting (Danese et al., 2022).

In order to search for elements to complement/support the interpretative hypotheses suggested by the archaeological evidence to reconstruct the ancient site of San Pietro Infine, a detailed analysis of LiDAR data made available by the National Geoportal (Ministry for the Environment, Land and Sea) of the Italian state was performed. The Italian state provides for free LiDAR data covering most of the peninsula. The data are provided by the National Geoportal, upon request, already processed as point clouds or DTMs, already filtered as only points belonging to the ground, and are distributed under a Creative Commons Attribution 3.0 license. According to the geo-portal of the Ministry, the information of PST (*Piano Straordinario di Telerilevamento*, Not-Ordinary Plan of Remote Sensing) PROJECT - LIDAR DATA were acquired with ALTM Gemini, ALTM 3100EA and Pegasus laser - scan systems of the Canadian Optech Company. These systems consist of one or two laser heads operating in the near-infrared (1064 nm) that send out light pulses at a frequency ranging from 33 kHz to 400 kHz depending on the flight altitude. The data from the aerial shots were statistically analyzed and classified for modelling using the Terra Match module of the TerraScan software from the Finnish company Terrasolid (http://www.pcn.minambiente.it/geoportal/catalog/search/resource/details.page?uuid=m_amte%3A299FN3%3A8740c0d0-8f32-4e85-9856-42f8b88853da, last accessed on February 12, 2023). DTM raster data at 1 m/pixel cell resolution was used for this study. The data provided by the Ministry were then processed to highlight micro-reliefs and topographic features of possible archaeological interest using the open source RVT (Relief Visualization Toolbox) v. 2.2.1 desktop tool (Kokalj et al., 2019).

The derived DTMs produced for this study are specified in Table 1 and showed in Fig. 3.

Then all the enhanced visualizations of DTM data were subsequently used within a GIS platform (QGis) in order to be interpreted from a purely archaeological point of view, in accordance with what is already known for the area of interest (Fig. 4).

In particular, it should be noted the identification of micro-reliefs that attest the presence, not found in the visible spectrum, of a road

Table 1
Derivatives based on visualization techniques.

Visualization method	Parameters
Hillshading	Sun azimuth (deg): 315; Sun elevation angle (deg): 35
Hillshading from Multiple directions	Number of directions: 16, Sun elevation angle (deg): 35
PCA of Hillshading	Number of components to save: 3
Slope gradient	No parameters required
Simple Local Relief Model	Radius for trend assessment (pixel): 5 and 10
Sky-View Factor	Number of search directions: 16, Search radius (pixel): 5 and 10
Openness – Positive	See above
Openness – Negative	See above
Archaeological VAT	General preset

with an east–west trend about 20 m south of the religious building (Id 8), which intersects with two probable parallel roads (Id 15 and 17) oriented approximately SW-NE (also these evidences are not found in the visible spectrum). Specifically, the road found in the east area (Id 15) is about 10 m from the church. Finally, the LiDAR visualizations confirm the presence of the large Roman building (Id 31), identified during the previous survey 80 m to S-E of the church, and allow us to read very well also the diverticulum of the *Via Latina* with trend NW-SE (Id 30). The micro reliefs Id 10, 16, 18 and 42, instead, given the proximity to the segment of the *Via Latina* and another probable road to the south with an E-W trend (Id 2), could be attributed to the remains of Roman mausoleums. Unfortunately, we have little data to propose certain reconstructive hypotheses on the evidences Id 1, 3, 4, 5, 6, 7 and 13.

3.2. Geophysical prospecting

Geophysical methods are certainly fundamental tools for the historical reconstruction of ancient sites without necessarily resorting to excavation work, due to their ability in identifying and characterizing buried features/structures attributable to anthropogenic remains. However, over the past decade, several studies have shown that the best benefits of such methodologies applied to the archaeological field come from their integration with information from remote sensing surveys and archaeological research (e.g., Křivánek, 2017; Di Maio et al., 2018; Deiana et al., 2020; Henry et al., 2020). In particular, for the present case study, a multimethodological geophysical prospecting was planned to support some of the interpretative hypotheses that emerged from the LiDAR data and the fragmentary information from historical, epigraphic, and archaeological sources. The aim is to investigate at medium to shallow depth the geological setting of the test site with the dual purpose of detecting geophysical anomaly patterns ascribable to the hypothesized *Ad Flexum* junction, and to identify possible geophysical lineaments attributable to buried anthropic remains of the village that historical sources assume developed around the church of San Pietro Infine. Specifically, high-resolution magnetic (MAG), frequency-domain electromagnetic (FDEM) and ground penetrating radar (GPR) surveys were carried out in a test area of size 100 × 100 m^2 (Fig. 5) surrounding the remains of the *Il Torrione*, composed of Roman and medieval building elements. The choice of the mentioned methodologies is based on the expected variation in the magnetic and electrical properties between targets and geological setting of the area, which are respectively formed by bricks and/or limestone materials and sandy, clayey or swampy soils (see Section 2.1). In fact, in archaeological research, magnetic anomalies are mainly generated by magnetic

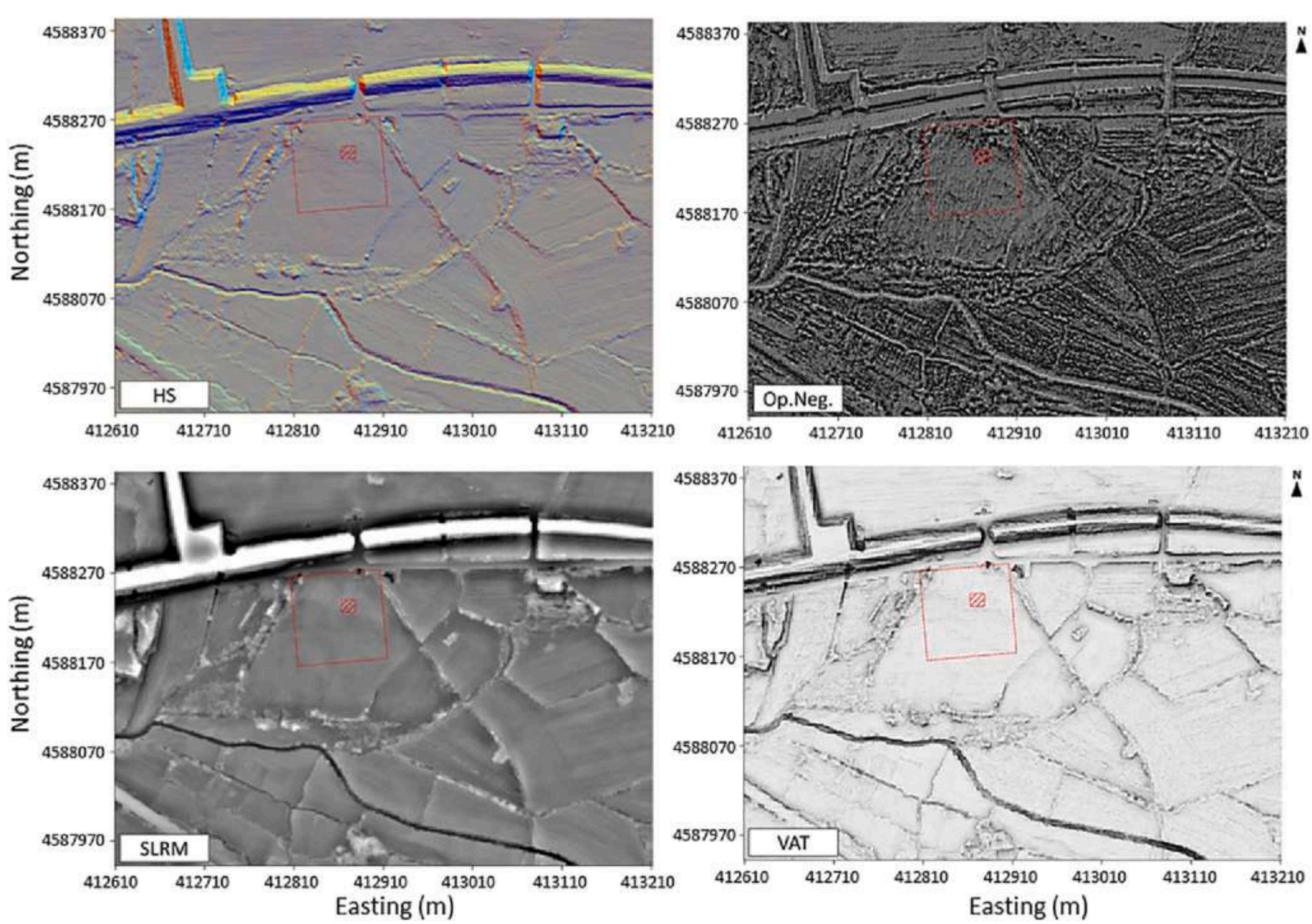

Fig. 3. Examples of enhanced visualisations of DTM: Multiple Hillshading, Openness Negative, Simple Local Relief Model, and Archaeological VAT.

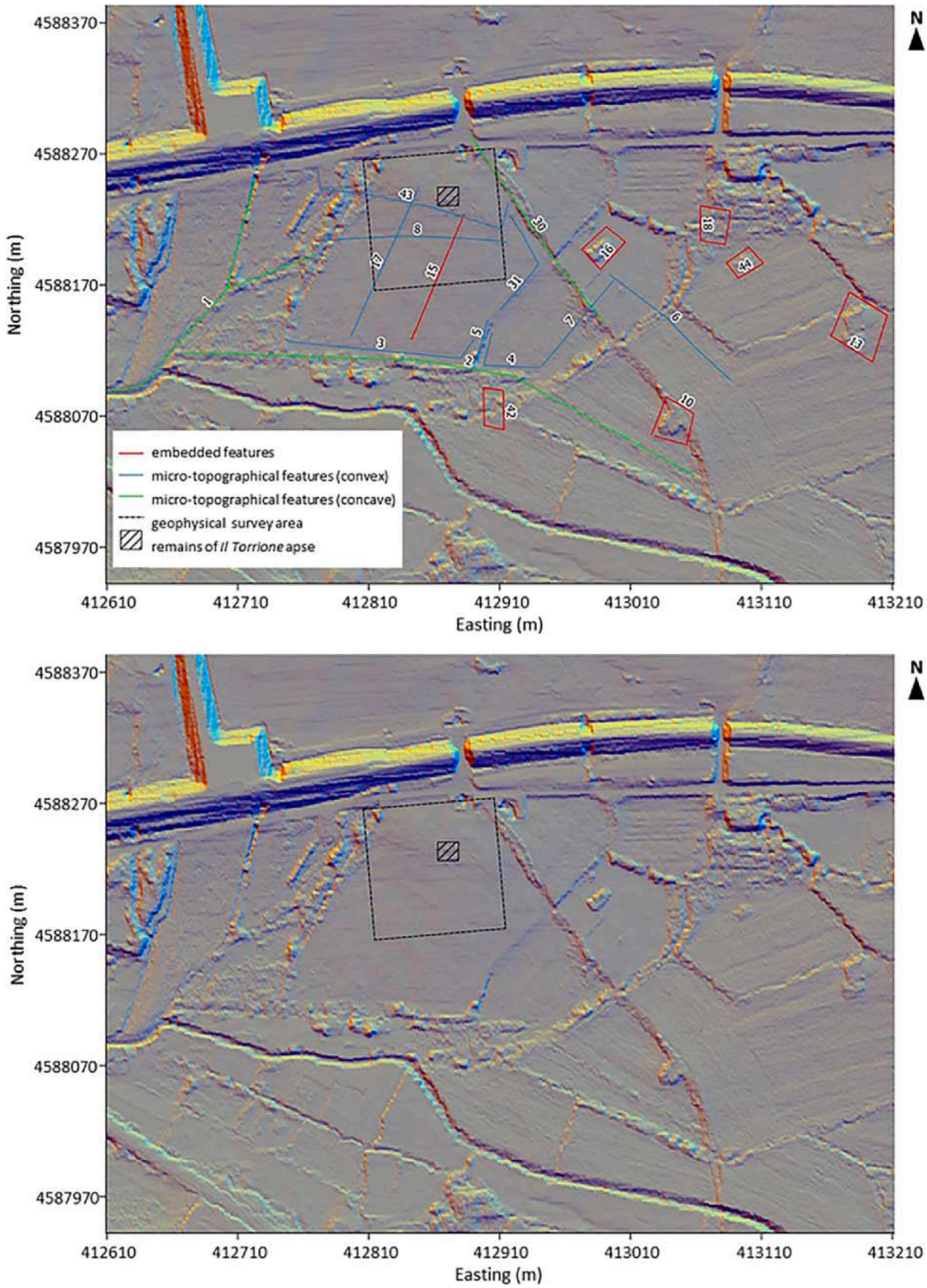

Fig. 4. (Top) Features of archaeological interest identified by the enhanced visualisations of DTM. The black rectangle indicates the geophysical survey area. Multiple Hillshading is used as background; (bottom) the top image without the archaeological and micro-topographical features.

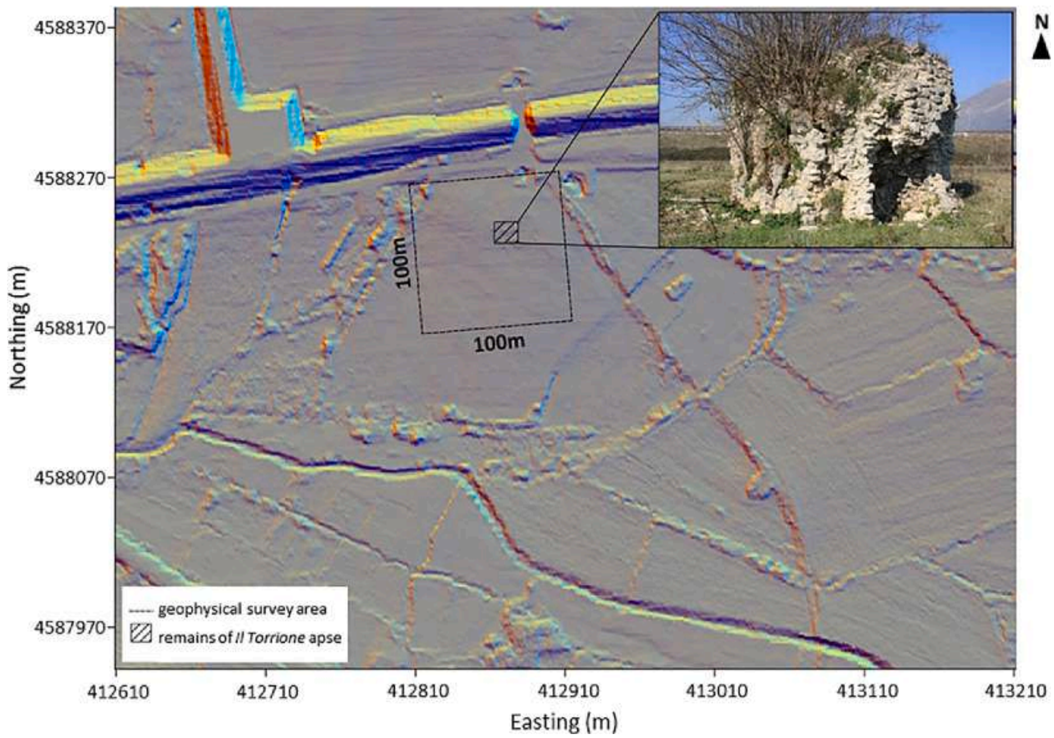

Fig. 5. Geophysical survey area and remains of *Il Torrione* apse. Multiple Hillshading is used as background.

susceptibility contrasts between artifacts and geological background (e.g., Aspinall et al., 2008; Di Maio et al., 2016; Ayad and Bakkali, 2018 among others). Moreover, their alignment, correlated with the distribution of the causative sources, provides information on the geometry and orientation of any buried anthropic remains (e.g., Arısoy et al., 2007; Gaffney, 2008). On the other hand, the occurrence of electrical anomalies, which identify areas with electrical properties different from the background, is indicative of hidden structures resistant to the passage of electric or electromagnetic signals, such as foundation walls, cavities, tombs, which are generally hosted in a more conductive environment due to the fluid circulation in the predominantly sedimentary coverages (e.g., Drahor et al., 2007; Di Maio et al., 2012; Saey et al., 2015; Di Maio et al., 2016; Yilmaz et al., 2019). First, MAG and FDEM surveys were performed for preliminary exploration of the study area to identify sectors characterized by meaningful contrasts in electrical and magnetic properties. Next, GPR measurements were carried out to better define any observed high-frequency MAG and FDEM anomalies, likely related to shallow and/or small-scale anthropic structures. The data were acquired along parallel profiles oriented approximately E-W and placed at a distance from each other comparable to the size of the structures to be detected (e.g., roads, walls, *stationes*, etc.), which is in the order of a few meters.

3.2.1. MAG survey

MAG is a widely applied passive geophysical method for mapping buried archaeological remains, due to its capability in detecting anomalies of the Earth's magnetic field induced by localized structures, such as walls, trenches, pits, graves, which therefore can be distinguished from the geological environment because of the magnetic contrast between the anthropogenic disturbance and the undisturbed soil (e.g., Silliman et al., 2000; Fassbinder, 2015; 2017 and references therein).

The MAG measurements in the survey area (black dashed rectangle in Fig. 5) were performed along parallel E-W profiles 0.5 m apart by the GSM-19 Overhauser Magnetometer (*GEM* System) in a gradiometric configuration. The latter enables to measure the vertical gradient of the Earth's magnetic field, which is given by the ratio of the difference in the field values recorded by two sensors placed at different heights from the ground level to their distance (vertical magnetic pseudo-gradient). This data acquisition mode allows the enhancement of high-frequency components of the signal generated by magnetic sources that are expected to be located at very shallow depths (e.g., Fassbinder, 2017). Based on preliminary tests aimed at finding a distance that would provide a high signal-to-noise ratio, the two used omnidirectional sensors were positioned at 1.70 m and 2.26 m from the surface level, respectively, i.e. at a distance of 0.56 m from each other. The data were acquired with a time interval of 0.5 s. Fig. 6a shows the vertical magnetic pseudo-gradient anomaly map obtained from the collected data, which highlights a generally low noise level of the acquired signals. Therefore, the data analysis focused mainly on reducing line effects between adjacent profiles, due to the bidirectional acquisition mode (i.e. roundtrip walking). The map, indeed, shows a typical "striping", defined as *heading error* (e.g., Scollar et al., 2009), which was reduced equalizing at the same mean value the data collected along each measurement profile (e.g., Scudero et al., 2018). Then, a DWT (Discrete Wavelet Transform) filter was applied to attenuate the "zigzag effect", again due to the bidirectional acquisition mode that can cause an offset between the position of the GPS system and the magnetic sensors (Ciminale and Loddo, 2001). Fig. 6b shows the magnetic map after data processing and filtering. A long-wavelength dipolar anomaly elongated in the NE-SW direction (A in Fig. 6b) is clearly evident in the central part of the investigated area; its shape and size could well account for the presence of the ancient buried Roman road (i.e., *Ad Flexum*, see Section 1). In contrast, the well-defined geometry of the smaller dipolar anomaly indicated by B in Fig. 6b suggests the presence of a wall structure. Moreover, the relatively large number of small-wavelength magnetic anomalies in the northern sector of the map compared to the southern one divides the survey area into two macro-sectors: one to the north, bordering the modern road that gives access to the site and probably related to an ancient rural settlement (i.e., *statio*, Zambardi, 2009b), and one to the south, likely used for agricultural and productive activities by virtue of its morphology and proximity to the watercourse.

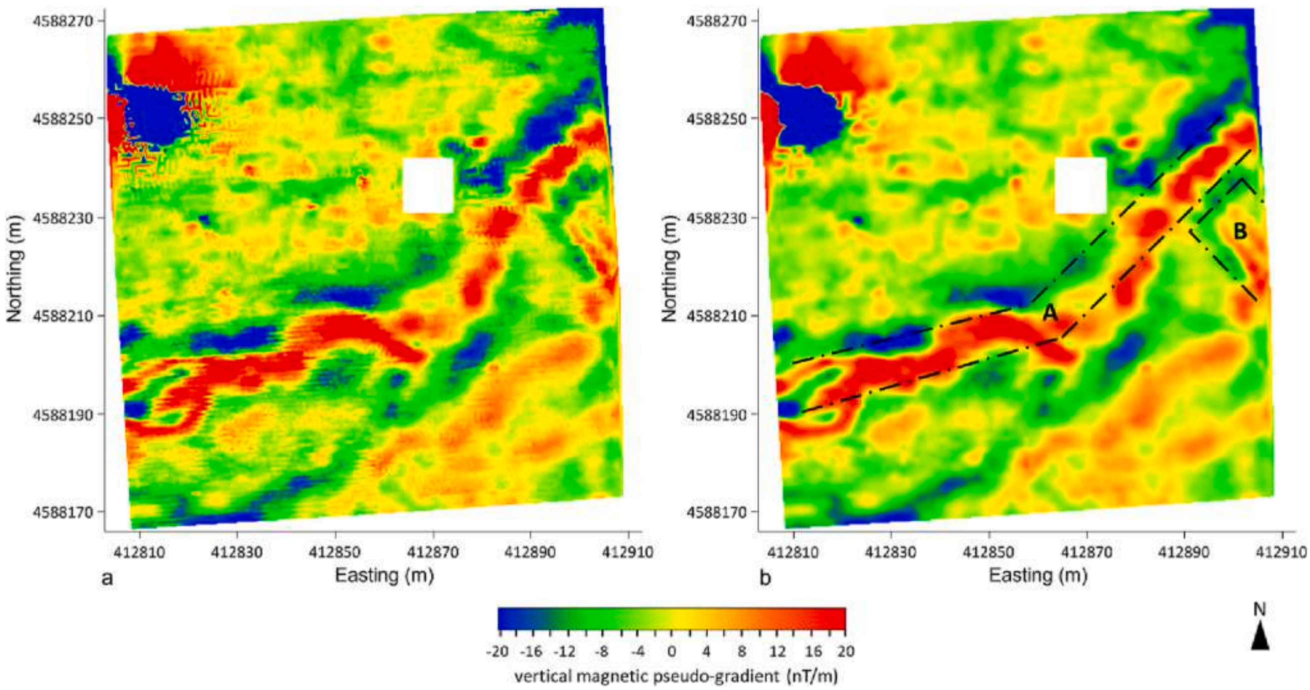

Fig. 6. Vertical magnetic pseudo-gradient anomaly map observed in the geophysical survey area (black dashed rectangle in Fig. 5) from (a) unprocessed data and (b) after reducing line effects between adjacent profiles. The white box indicates the position of the *Il Torrione* apse remains. The black dashed lines in (b) mark the main detected anomalies of archaeological interest.

3.2.2. FDEM survey

FDEM is an active geophysical method based on the induction of electrical currents in the subsurface by a primary electromagnetic field generated by passing an alternating current, at a specific low frequency, through a transmitter coil placed on the surface. This field induces eddy currents in the conductive materials traversed by the primary field, which in turn generate a secondary field. The latter is recorded, along with the primary field, by a receiver coil placed at a fixed distance from the transmitter coil and returned in terms of in-phase and out-of-phase (or quadrature) components against the primary field, usually expressed in parts per million (ppm) (e.g., Reynolds, 2011). The former component is related to the presence of magnetically susceptible materials/structures in the subsurface, while the latter is directly related to the ground electrical conductivity (e.g., McNeill, 1980; Won and Huang, 2004; Christiansen et al., 2016). The application of the FDEM method in archaeology is now widespread due to its ability to provide a quick characterization of large areas in terms of distribution of electric and magnetic parameters, whose possible variations are determined by contrasts in the physical properties of buried archaeological features compared to the host soils (e.g., De Smedt et al., 2013; Di Maio et al., 2016; Pueyo Anchuela et al., 2016; Deiana et al., 2022). In particular, it is generally supplemented with magnetic survey to investigate sites where magnetic susceptibility contrasts are suspected to be too low to be detected (e.g., an alluvial geological setting hosting limestone wall remnants), while high contrasts in the electrical properties are assumed to exist (e.g., limestone materials hosted by a generally conductive sedimentary environment). However, due to the lower resolution and penetration depth compared to high-resolution and/or relatively deep survey methods, such as GPR and/or geoelectrical surveys, it is generally used in conjunction with these methods, rather than alternative to them (e.g., Pavoni et al., 2021).

The FDEM data at the San Pietro Infine test site (black dashed rectangle in Fig. 5) were recorded along parallel E-W profiles 1 m apart by using the Profiler EMP-400 multi-frequency electromagnetometer (GSSI, Nashua, USA). It consists of two coils (transmitter and receiver) separated by a fixed distance of 1.21 m and is able to simultaneously investigate up to three selected frequencies in the range 1–16 kHz. Based on results obtained at other archaeological sites characterized by geological contexts similar to the one studied in this paper (e.g., Di Maio et al., 2016), the three frequencies 1, 10 and 15 kHz were chosen, which should allow for accurate exploration of the first few meters of the subsurface by using a vertical coplanar coil orientation (Saey et al., 2012). The acquired FDEM data (in-phase and out-of-phase components) were manually despiked to remove data likely contaminated by ambient noise, and then leveled against a zero level by calculating the arithmetic mean of the survey data and subtracting that value from the dataset (e.g., Delefortrie et al., 2018; Miller et al., 2019). Fig. 7 show the distribution of the in-phase and out-of-phase component values of the induced magnetic (secondary) field after the data processing for all the three investigated frequencies. The maps in Fig. 7a, b and c show, for all frequencies, an anomalous distribution of the in-phase values fully consistent with the magnetic anomaly map in Fig. 6b. In fact, the central sector of the area is dominated by a sharp anomaly characterized by low values of the in-phase component, whose shape and orientation correspond well with the large anomaly pattern observed in the magnetic map, thus providing further support for the identification of the *Ad Flexum* paved road. Furthermore, the maps in Fig. 7d, e and f show a clear separation in the distribution of the out-of-phase component values; in fact, the N-NE sector is characterized by quadrature values lower than those observed in the western sector. This trend is clearly visible in the higher frequency maps (i.e., 15 kHz and 10 kHz), which correspond to shallower exploration depths, while it is much less marked in the 1 kHz frequency map, which includes contributions from natural and/or anthropic anomaly sources located at greater depths. Considering that the quadrature component is directly proportional to the apparent electrical conductivity of the investigated subsurface volume (McNeill, 1980), it is realistic to correlate the low quadrature values observed in the NE sector with the presence of buried anthropogenic structures, whose resistivity is assumed to be higher than the relatively conductive host environment (see Section 2.1). The sharp increase in the out-of-phase values observed in the N-NE sector of the lower frequency map (1 kHz, Fig. 7f) would support this interpretive hypothesis. Indeed,

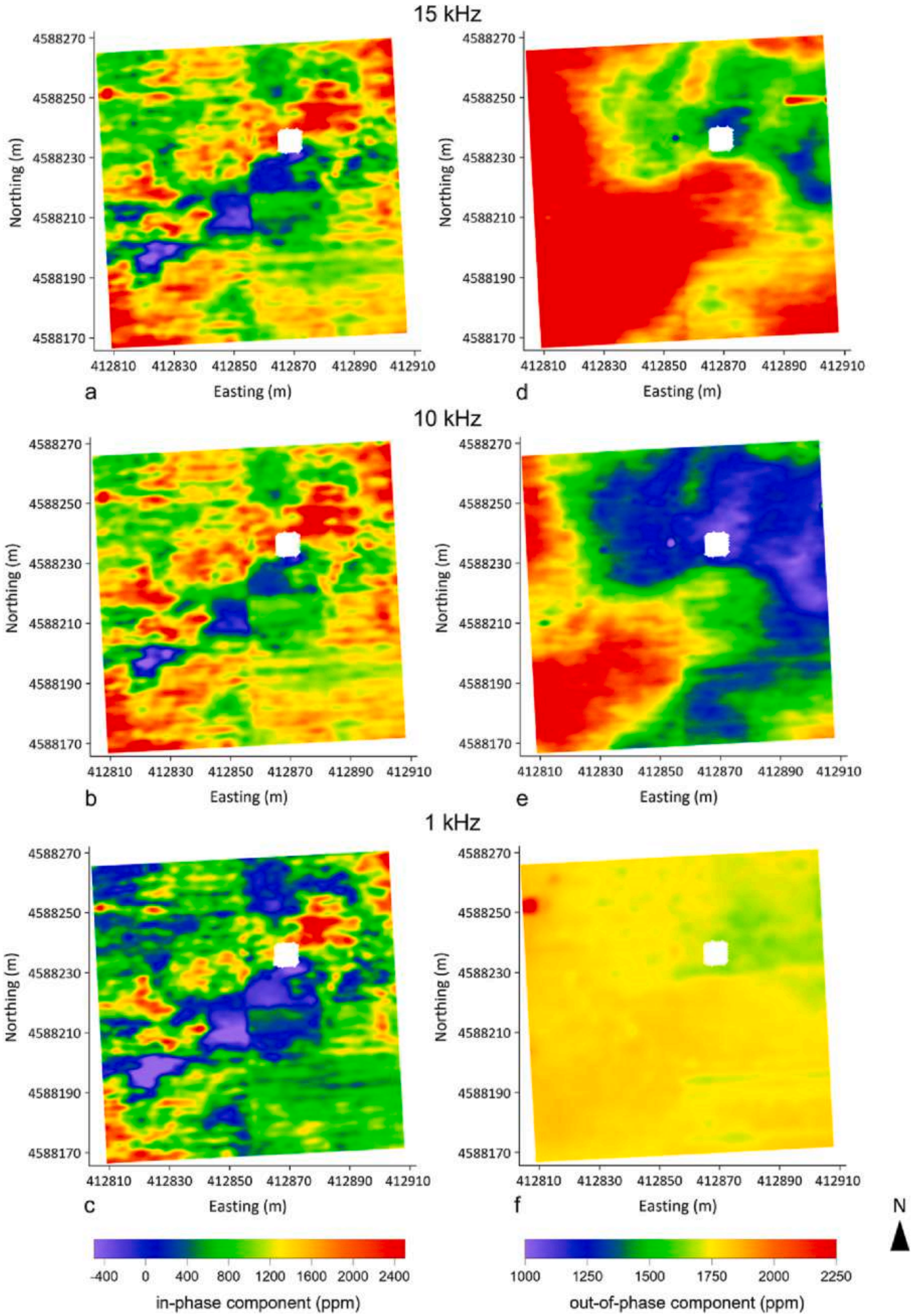

Fig. 7. Maps of the in-phase (a, b, c) and out-of-phase (d, e, f) components provided by the FDEM prospecting in the geophysical survey area (black dashed rectangle in Fig. 5). The white box indicates the position of the *Il Torrione* apse remains.

it is reasonable to assume that at greater depths the largest contribution to the observed quadrature values comes from the deepest source(s), which in this case would be the geological formations. Therefore, the quadrature component maps also provide evidence to support the inferences drawn from the magnetic data interpretation (Fig. 6b), namely the presence of buried remains ascribable to an ancient rural settlement in the northern sector of the survey area. It is worth noting that the different geological characteristics of the explored subsurface could also contribute to a lowering of the out-of-phase component in the north-eastern part of the investigated area. The latter, in fact, might be characterized by sandy soils free of clayey materials, in contrast to the south-western sector, which might instead correlate well with a marshy environment with clayey fractions, based on the periodic overflows of the river rod flowing south of the area.

3.2.3. GPR survey

GPR is one of the most common active methods used in archaeological research due to its high resolution for near-surface investigations (Conyers, 2016 and references therein). It aims at identifying possible dielectric contrasts between buried anthropic structures and host soils by transmitting high-frequency radar pulses in the ground and recording amplitude and delay time of the reflected pulses as they encounter discontinuities in the dielectric properties of the media traversed by the radar pulse (e.g., Davis and Annan, 1989). A GPR system is configured as mono or bi-static; in the former case, a single antenna serves as both transmitter and receiver, while in the latter configuration the transmitting and receiving antennas are separate. Exploration depth and spatial resolution are closely dependent by the frequency of the emitted signal and the type of material to investigate. GPR works typically in the frequency range 100 MHz − 2 GHz: the higher the frequency, the greater the vertical resolution, but the lower the penetration depth. The GPR response is generally visualized in terms of radargrams, which are two-dimensional maps showing the increasing delay-time from the initial impulse for each position of the radar antenna on the ground surface. In the archaeological field, the surveys are generally performed according to 3D geometries to capture the three-dimensional shape of any buried remains (Leckebusch, 2000; Grinc, 2015; Leucci et al., 2016). In this case, the data are acquired along parallel profiles about 0.5 m apart and represented in terms of horizontal maps (time slices) of the reflection amplitudes, which are extracted at various reflection times from the entire dataset (e.g., Leucci et al., 2016 among others). By estimating the average propagation velocity of the radar wave in the subsurface, it is then possible to convert the time slices in depth slices, which highlight the possible radar structures within the investigated volume. For archaeological investigations, the diffraction hyperbola fitting method is generally used to retrieve the average propagation velocity (e.g., Wolff and Urban, 2013). The method compares synthetic hyperbolas with known velocities to the hyperbolas displayed in the experimental radargrams until the true velocity is found.

The GPR survey at the San Pietro Infine test site was carried out according to a 3D geometry along the same profiles of the MAG prospection by using the SIR-3000 radar system (GSSI, Nashua, USA) equipped with a 400 MHz monostatic antenna. The data were acquired using a space sampling of 0.016 m, a time window of 60 ns, and the manual gain function. Due to low-level noise on the acquired reflected signals, the data were processed with the Reflexw 7.0 Sandmeier software by applying basic processing techniques, specifically static correction, temporal filtering, and background removal (e.g., Yilmaz, 1987). As an example, Fig. 8b shows six radargrams along some profiles located in the northern sector of the survey area (Fig. 8a), where the main GPR anomalies were identified. As can be seen, an investigation depth of approximately 2.5 m below ground level (b.g.l.) was achieved by using an average radar signal propagation velocity of 0.12 m/ns for time-to-depth conversion. High-amplitude reflections of the radar signal are mainly visible in the N-E sector from about 0.4 m depth (red arrows in Fig. 8b). The hyperbolic shape and size of the observed GPR

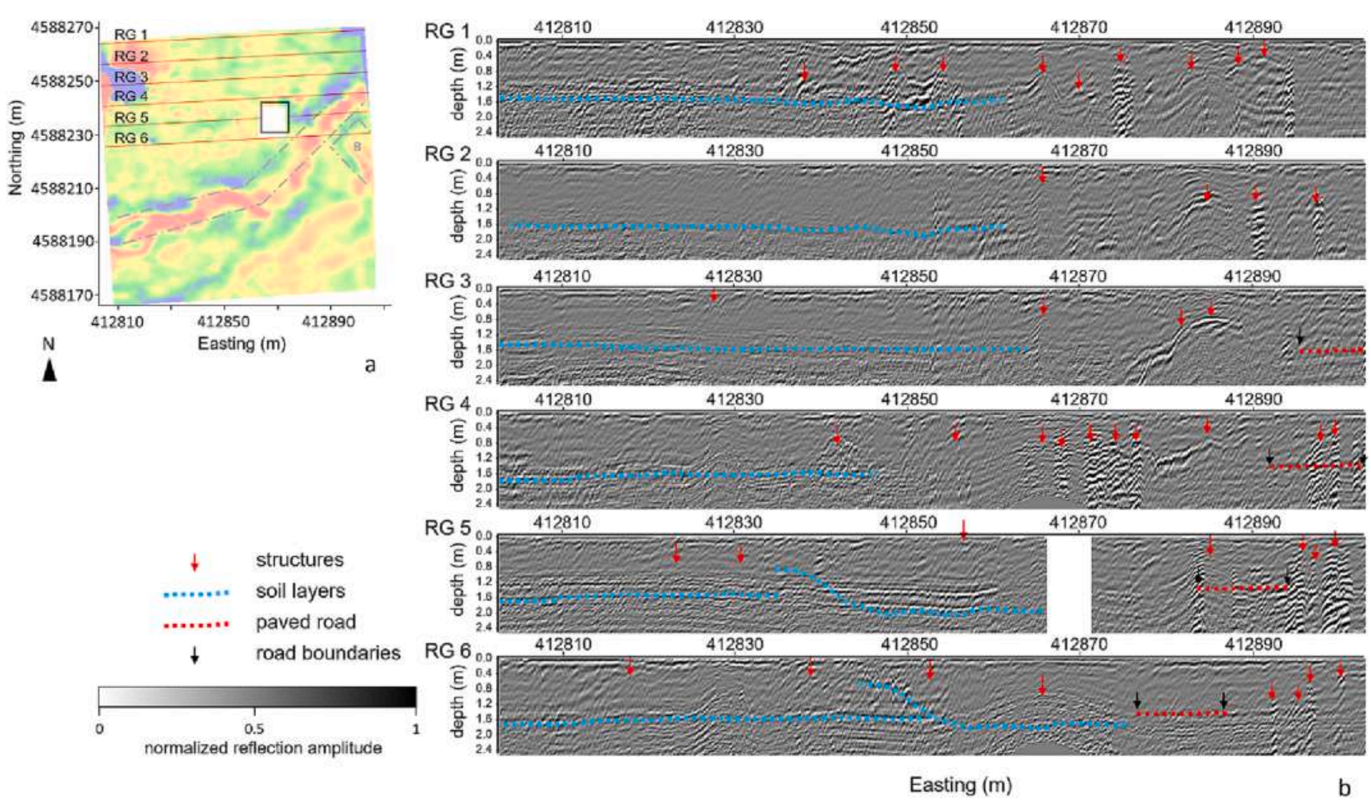

Fig. 8. a) Location of the selected GPR profiles (RG 1 – RG 6) 8 m apart. The open black box indicates the position of the *Il Torrione* apse remains. The magnetic map in Fig. 6b is used as a background to facilitate comparison with the observed GPR anomalies. b) Processed GPR radargrams along the six profiles RG 1 – RG 6. The symbols outline the main detected reflectors.

anomalies correlate well with the presence of reflectors due to anthropic buried structures. Continuous horizontal reflectors are also evident mainly in the N-W sector (blue dotted lines) at a depth of approximately 1.6–1.8 m b.g.l., sometimes interrupted by gentle and extensive inclined reflectors, probably due to soil stratification. Based on the geological setting of the study area (see Section 2.1), the relatively low amplitude of the observed reflections may be an indicator of the interface between alluvial soil and sand-silty substrate, likely a Roman paleosoil. Interestingly, in the easternmost part of the RG 3, 4, 5 and 6 radargrams, the high-amplitude GPR anomalies are interrupted, at a depth of about 1.5 m b.g.l., by a narrow horizontal reflector (red dotted lines) corresponding approximately to the trace of the *Ad Flexum* paved road (see its trace on the background magnetic map in Fig. 8a), as suggested by the results of the MAG and FDEM surveys. We note that, along the radargrams RG 3 and 4, this horizontal trend seems to be influenced by the reflections from the remains of anthropic structures of the medieval village, probably built around the church. All the processed radargrams (see examples in Fig. 8b) showed the presence of vertical features, which were often consistent between successive profiles. In order to better enhance their lateral continuity, time slices were extracted from the whole GPR data volume, with a vertical integration of 3.0 ns, to investigate the distribution of the reflection amplitude values in maps parallel

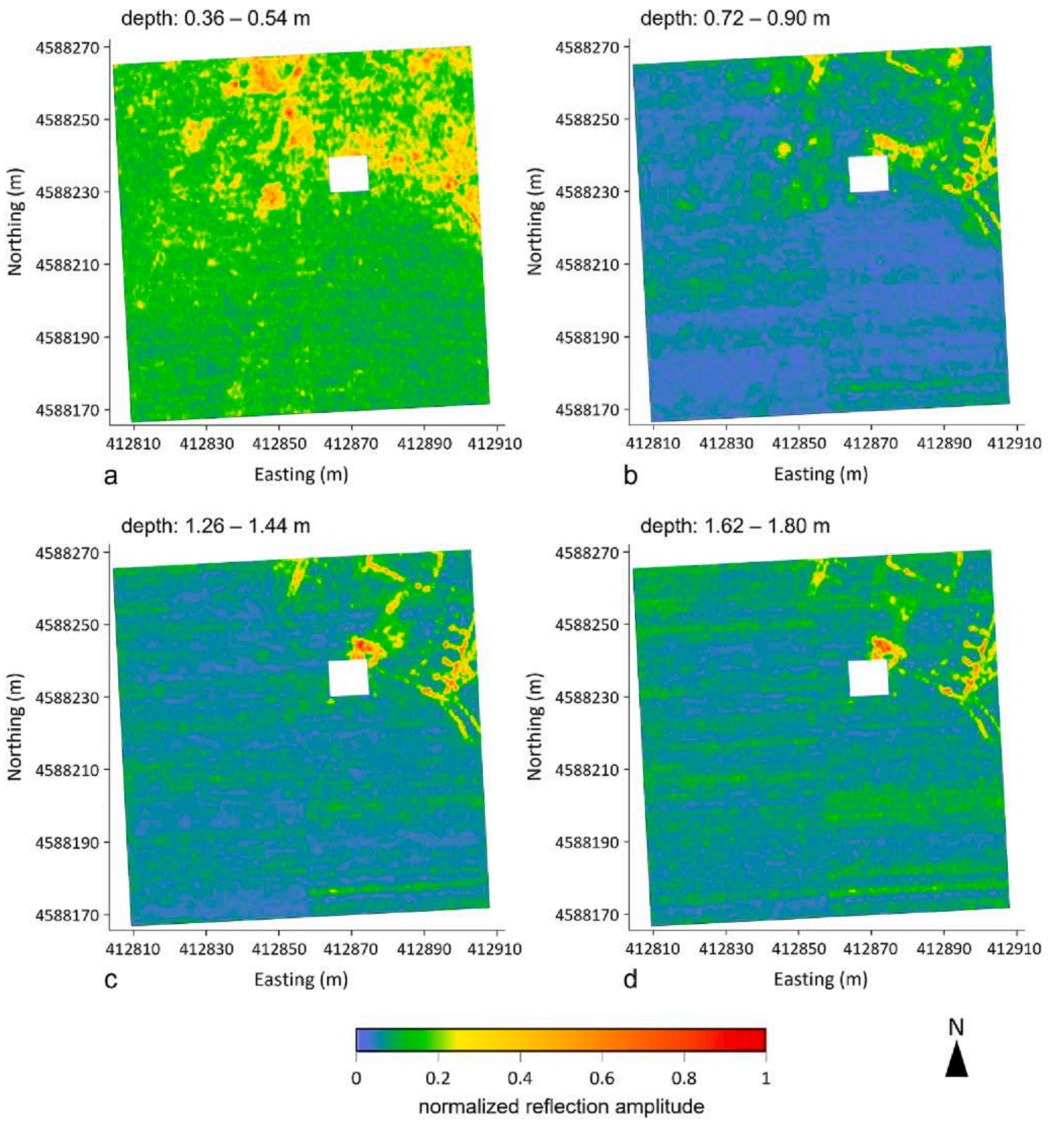

Fig. 9. Depth slices provided by the GPR prospecting in the geophysical survey area (black dashed rectangle in Fig. 5) for different depth intervals from the surface level. The white box indicates the position of the *Il Torrione* apse remains.

to the ground surface, then converted in depth slices using the average radar signal velocity of 0.12 m/ns. Fig. 9 shows the depth slices selected at different depth intervals to highlight the main observed GPR anomalies within the explored volume. As expected by the analysis of all the radargrams, linear geometries of high-amplitude GPR-reflections ascribable to the presence of anthropic structures are identified in the N-E sector of the maps from a depth of about 0.4 m b.g.l. (Fig. 9a), although embedded in a rather noisy background. Such anomalies, which begin to be clearly defined at greater depth (Fig. 9b) and visible up to about 1.8 m b.g.l. (Fig. 9d), correlate well with the small wavelength magnetic anomalies visible in the same sector (Fig. 6b) and attributed to wall-like structures. The lack of significant anomalies in the remaining part of the maps in Fig. 9 is probably ascribable to the geological characteristics of the south-western sector of the investigated area, which, based on the results provided by the other survey methodologies, would consists of marshy soils with clayey material. The nature of the subsurface would, therefore, be responsible for the significant absorption of the GPR signal observed at all depth ranges. Finally, we note that the distribution of the high-amplitude anomalies helps to trace the development of the village, which probably developed around the religious building, thus supporting the interpretative hypotheses derived from the MAG and FDEM surveys. Furthermore, the depth extension of these elongated anomalies is consistent with the depth of the Roman paleosoil inferred from the radargram analysis.

4. Integrated interpretation of LiDAR, geophysical and archaeological outcomes

Fig. 10 shows the map of the *Ad Flexum* site that integrates the lineaments identified by the LiDAR survey with the results of the multi-methodological geophysical prospecting. As can be seen, LiDAR data not only confirm the traces highlighted by the geophysical survey, but also allow them to be contextualized in a much wider area. Specifically, the long-wavelength magnetic anomaly asserted to the *Ad Flexum* paved road (see Section 3.2.1) fits very well with the trace detected by the LiDAR analysis (Id 15 in Fig. 10a), although the latter does not highlight the flex, i.e. the *Ad Flexum* junction, which is instead clearly visible from the vertical magnetic pseudo-gradient map. This apparent mismatch could be due to degradation of the slope in a S-W direction, i.e. toward the river, where the alluvial deposits may have covered over time the traces that were previously visible on the surface. This hypothesis is further supported by the results of the FDEM survey, which suggest that the south-western part of the investigated area could correlate well with a marshy environment with clayey fractions, due to periodic overflows of the river channel (see Section 3.2.2 and Fig. 7d, e). Furthermore, the arrangement of the high-amplitude GPR anomalies in the N-E sector (Fig. 10c), which correspond well to the high-frequency magnetic anomalies observed in the same sector (Fig. 10a), appears to be interrupted by both the LiDAR lineament Id 15 and the large-wavelength magnetic anomaly (Fig. 10c). Position, shape, and reflection amplitude of the GPR anomalies could be tentatively attributed to the masonry structures that probably constituted the *statio* located on opposite sides of the *Ad Flexum* main road. Finally, we note that the in-phase component map from the FDEM survey shows anomaly patterns consistent with the two parallel paths, oriented approximately SW-NE, assumed from the LiDAR data analysis (Id 15 and 17 in Fig. 10b).

To provide further support for the hypotheses resulted from the integrated interpretation of the LiDAR, geophysical and archaeological findings, a forward modeling of the magnetic data was performed by assuming the presence of buried prismatic sources with direction of magnetization parallel to the ambient magnetic field (i.e. declination 3.7° and inclination 58°). Fig. 11 shows the synthetic map of the vertical magnetic pseudo-gradient related to sources whose position, size and magnetic contrasts with the surrounding soil have been chosen according to the results from the high-resolution GPR survey, the LiDAR data analysis and the characteristics of the remains found in the study area, made of marble, limestone and tiles. With reference to the assumed distribution of the magnetic sources, the long-wavelength dipolar anomaly in the central part of the investigated area (A in Fig. 6b) is well reproduced by two sources, approximately 6 m wide by 65 m long, with the top at a depth of 1.5 m b.g.l., characterized by a positive magnetic contrast with the surrounding soil. Size and depth of such a structure are consistent with those of a road made of calcareous paving stones, whose position seems to correspond with the *Ad Flexum* junction. Furthermore, the distribution of the magnetic anomalies that characterizes the north-eastern sector of the study area (B in Fig. 6b), which compares well both in shape and extent with that of the GPR anomalies (Fig. 9) observed in the same sector, is instead well reproduced using seven smaller prismatic sources (approximately 1–2 m wide and 3–15 m long) characterized by different azimuths and positive or negative magnetic contrasts with the background. Although top depth and thickness of these structures are approximately the same as those used to model the long-wavelength anomaly, it was necessary to use magnetic contrasts that were generally about an order of magnitude lower in order to achieve a good match between the synthetic and observed magnetic data. This suggests the presence of wall remains (e.g., inconsistent mixed masonry made of limestone, brick, and *pisé*) according to the building materials used in the Roman period.

5. Discussion and conclusions

Integrated interpretation of LiDAR and geophysical data allow us to profile with greater clarity the complex settlement reality that characterizes the *Ad Flexum* archaeological site. First of all, we can confirm the continuity of activity of this area from the Roman period to the Middle Ages. The persistence of roads that across the area makes this territory of crucial importance, although, with the information available to us, it is impossible to assume a certain chronology of the traces and/or structures identified from the interpretation of the LiDAR and geophysical data. The extent of the structures might suggest the presence of an early medieval village developed around the religious building. The church of San Pietro belongs to the property of Montecassino Abbey, i.e. a 6th-century monastery located southeast of Rome (central Italy), and is mentioned in a lawsuit in which the boundaries of the lands, donated by Gisulfo and unfairly occupied by the gastald Guiselgardo, are reported (Gattula, 1734). The intervention of the abbot of Montecassino suggests the importance of these lands and the probability that the church of San Pietro also had the function of managing these lands. In addition, the hypothesis of a village in the vicinity of a religious rural building should not be surprising. In the early Middle Ages, in fact, it was monastic communities that probably gave rise to some villages. We can recall, for example, the case of San Martino di Ruviano (Caserta, southern Italy) connected to the homonymous cell of Montecassino, known from the early 9th-century and equipped with lands, houses and a *curtis* (rural farm) (Gattula, 1733; CMC, 1980; Esposito, 2010), and the Vicus Bonelle, pertaining to the abbey of S. Maria in Cingla (also a Montecassino cell) and probably located to the north in the Municipality of Ailano (Caserta) (Gattula, 1733; CMC, 1980; Bloch, 1986). Therefore, it is very likely that the identified traces are also pertinent to the presence of a village organized around the church of San Pietro. This village may have housed a small community of farmers who worked the lands of Montecassino. This abbey, in fact, had an obvious interest in garrisoning a crucial area crossed by important roads of *Langobardia Minor*.

It should be noted, however, that although our study suggests the presence of an early medieval village, the case of San Pietro Infine cannot be traced back to a precise settlement model. Indeed, at the present stage of research, only a few late antique and early medieval villages in Italy are known and studied through archaeological excavations, in many cases attested only by the discovery of ceramic material and a few traces of buildings. There are therefore no regional models applicable to all contexts, partly because the historical events that affected the Italian countryside in the early Middle Ages differed from

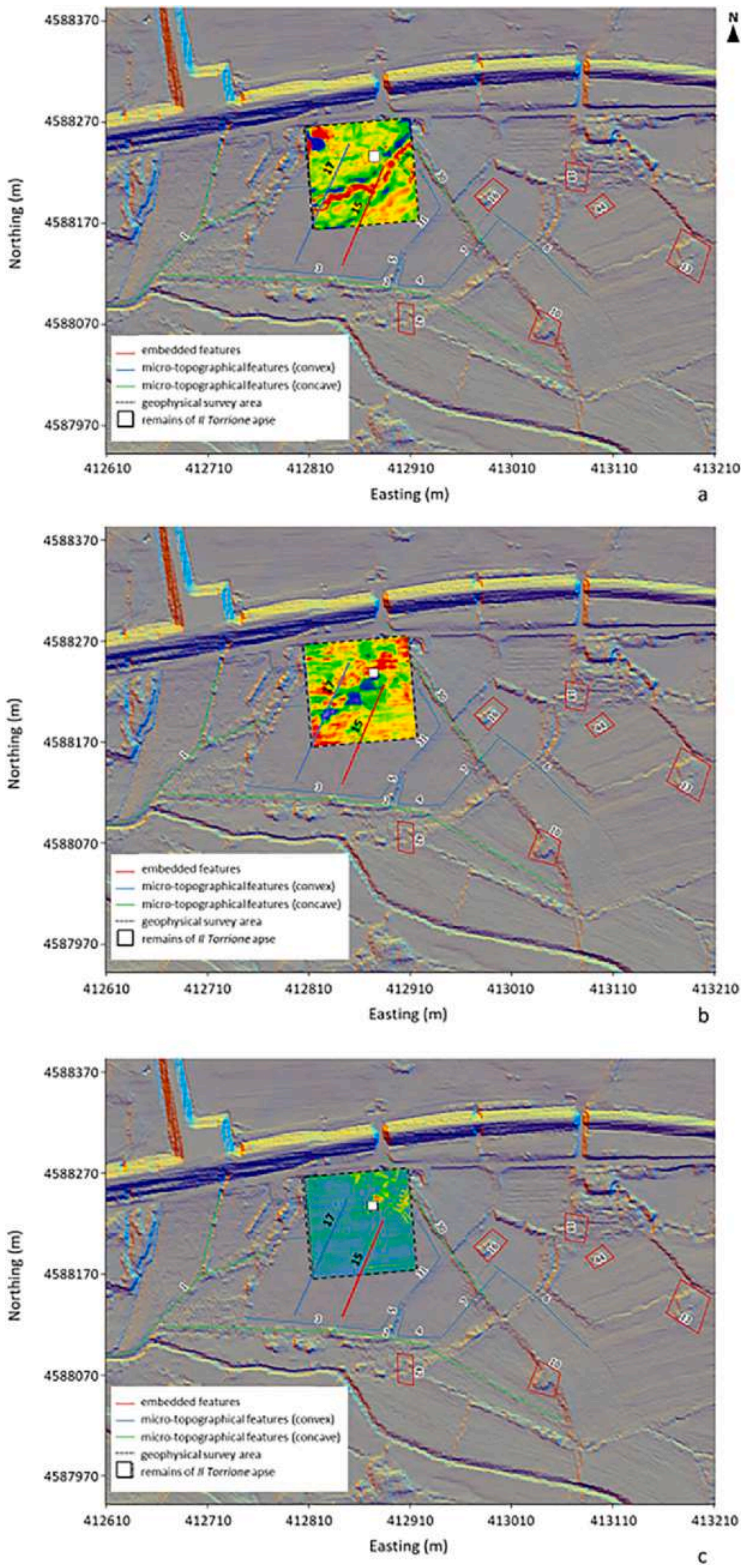

Fig. 10. Map of the *Ad Flexum* area that integrates the LiDAR traces with the vertical magnetic pseudo-gradient anomaly map (a), the in-phase component map at 10 kHz from the FDEM survey (b), and the depth slice in the range 1.21–1.35 m from the GPR survey (c).

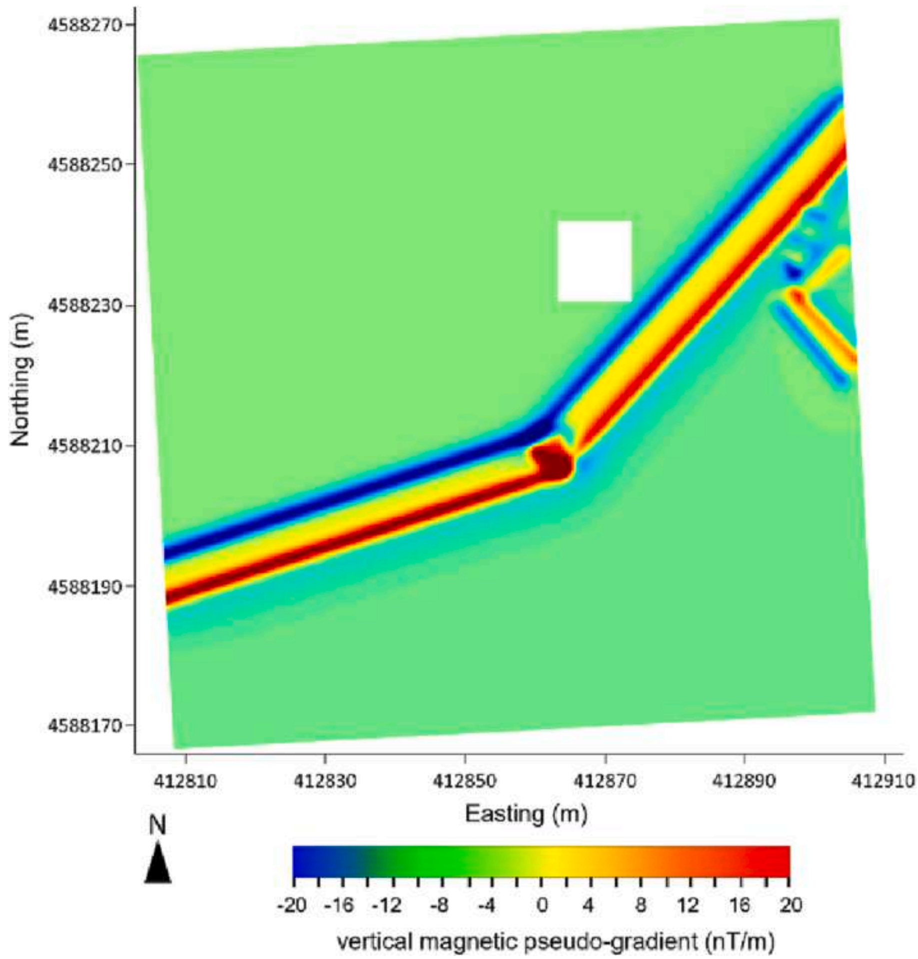

Fig. 11. Synthetic map of the vertical magnetic pseudo-gradient generated by buried prismatic sources with direction of magnetization parallel to the ambient magnetic field (see text for details).

region to region. However, it is reasonable to assume that the settlement of San Pietro Infine, similarly to other cases in Italy, was a village with small wooden and mixed-technology dwellings around a small church and a cemetery, a few buildings used for productive activities and surrounding fields for cultivation. In Piemonte (northern Italy), i.e. where *pagi* and *vici* are as widespread as in Lazio and Campania regions, the case of Collegno (Torino) can be cited. There, stratigraphic studies have shown that the Late Antique village (with wooden buildings on masonry foundations), originating from a Late Roman settlement, developed in the Lombard period and moved towards the river in the 11th century, in an area where a church is attested. With regard to southern Italy, where the archaeological site of San Pietro Infine is located, the written sources are rather ambiguous and the settlements that have been archaeologically investigated are few and have rather different characteristics. It is therefore still difficult to say what the villages were like between the 9th and early 12th centuries (Loré, 2012). The exception is Abruzzo, where several late antique and early medieval settlements are known thanks to the discovery of pottery areas or the presence of cemeteries linked to churches, or even the transformation of Roman *vici* and *villae* (Staffa, 2006). Among the excavated sites is the settlement of Moscufo (Pescara), whose occupation periods are very similar to those of San Pietro Infine. It is, in fact, the Cassinese women's monastery of St. Scolastica, located near an area where a section of the *Via Flaminia* crosses the Tavo River. Pottery fragments and several masonry structures in *opus incertum*, attributable to a Roman settlement later reused in the Early Middle Ages, were found in the area. The village of Colle S. Giovanni, near Atri (Teramo), was also built on an earlier Roman site, with raw earth houses near the church and pits dug in the ground to store foodstuffs (Staffa, 2006). In Campania, several ancient villages founded along the main river valleys of the Paestum plain (Salerno) are known. Some are linked to the presence of monastic cells belonging to San Vincenzo al Volturno (Isernia), such as that of San Vincenzo in loco Tusciano (in the plain between the Sele and Calore rivers). In this case, archaeological research has confirmed the presence of a rustic *villa* dating back to the 1st-2nd century CE, with structures reused from a medieval settlement that was in use until modern times (Fiorillo, 2012). Another partially investigated fluvial village is that of San Lorenzo di Altavilla Silentina (Salerno) (with an early phase dated between the 6th and 7th centuries CE), which, like San Giovanni di Pratola Serra (Avellino), is one of the sites that originated in the vicinity of late-Roman farmsteads. In both cases, however, the only evidence of the existence of the village is the discovery of a cemetery (Peduto, 1984).

The case of San Pietro Infine offers, with the current study, an interesting example of another possible early medieval village associated with the presence of a monastic cell and the management of the surrounding land. In an area where archaeology has never studied these rural settlements, the data presented in this paper provide useful indications for starting a targeted archaeological investigation.

Declaration of Competing Interest

The authors declare that they have no known competing financial interests or personal relationships that could have appeared to influence the work reported in this paper.

Data availability

Data will be made available on request.

Acknowledgements

The authors thank the Editor and two anonymous Reviewers for their insightful comments and suggestions, which were very helpful in improving the manuscript.

References

Adamopoulos, E., Rinaudo, F., 2020. UAS-Based Archaeological Remote Sensing: Review, Meta-Analysis and State-of-the-Art. Drones 4, 46. https://doi.org/10.3390/drones4030046.

Arısoy, M.Ö., Koçak, Ö., Büyüksaraç, A., Bilim, F., 2007. Images of buried graves in Bayat, Afyon (Turkey) from high-resolution magnetic data and their comparison with preliminary excavations. J. Archaeol. Sci. 34, 1473–1484. https://doi.org/10.1016/j.jas.2006.11.005.

Aspinall, A., Gaffney, C., Schmidt, A., 2008. Magnetometry for Archaeology. AltaMira Press, Walnut Creek, CA, p. 208.

Ayad, A., Bakkali, S., 2018. Analysis of the magnetic anomalies of buried archaeological ovens of Aïn Kerouach (Morocco). Int. J. Geophys. 9741950. https://doi.org/10.1155/2018/9741950.

Banaszek, Ł., 2013. LiDARchaeology. Airborne laser scanning of the forested landscapes around Polanów (Pomerania, Poland). In: Z. Czajlik, A. Bödőcs (Eds.): Aerial Archaeology and Remote Sensing from the Baltic to the Adriatic, Institute of Archaeological Sciences, Faculty of Humanities, Eötvös Loránd University, 31-36.

Bloch, H., 1986. Monte Cassino in the Middle Ages. Edizioni di Storia e Letteratura, Roma (Italy), p. 1554.

Briese, C., Pfeifer, N., 2001. Airborne laser scanning and derivation of digital terrain models. In A. Grün & H. Kahmen (Eds.): *5th Conference on Optical 3D Measurement Techniques*, 80-87, http://hdl.handle.net/20.500.12708/43019.

Caiazza, D., 1995. Archeologia e storia antica del mandamento di Pietramelara e del Montemaggiore: Età romana, Vol. 2., Banco Popolare Nicolò Monforte Pietramelara (Italy), 510 pp.

Calzolari, M., 2003. L'Italia e l'Etruria nella Tabula Peutingeriana. In: F. Prontera (Ed.): *Vie e luoghi dell'Etruria nella Tabula Peutingeriana*, Leo Olschki Editore, Firenze (Italy), 43-52.

Carettoni, G.F., 1940. Casinum (presso Cassino). Regio I - Latium et Campania, Roma (Italia Romana: municipi e colonie, Ser.1,2).

Chase, A.F., Chase, D.Z., Weishampel, J.F., Drake, J.B., Shrestha, R.L., Slatton, K.C., Awe, J.J., Carter, W.E., 2011. Airborne LiDAR, archaeology, and the ancient Maya landscape at Caracol. Belize. J. Archaeol. Sci. 38, 387–398. https://doi.org/10.1016/j.jas.2010.09.018.

Christiansen, A.V., Pedersen, J.B., Auken, E., Søe, N.E., Holst, M.K., Kristiansen, S.M., 2016. Improved geoarchaeological mapping with electromagnetic induction instruments from dedicated processing and inversion. Remote Sens. 8, 1022. https://doi.org/10.3390/rs8121022.

Ciminale, M.A., Loddo, M., 2001. Aspects of magnetic data processing. Archaeol. Prospect. 8 (4), 239–246.

CMC I, 28, 1980. Chronica Monasteri Casinensis. Ed. by H. Hoffmann, "Die Cronik von Montecassino" in M.G.H. SS. XXXIV, Hannover.

Cohen, A., Klassen, S., Evans, D., 2020. Ethics in Archaeological Lidar. J. Comput. Appl. Archaeol. 3, 76–91. https://doi.org/10.5334/jcaa.48.

Conyers, B.L., 2016. Ground-Penetrating Radar for Geoarchaeology. Wiley Blackwell, p. 160 pp..

Corns, A., Shaw, R., 2009. High resolution 3-dimensional documentation of archaeological monuments & landscapes using airborne LiDAR. J. Cult. Herit. 10, e72–e77. https://doi.org/10.1016/j.culher.2009.09.003.

Costa-García, J., Fonte, J., Blanco, A., González-Álvarez, D., Gago, M., Blanco-Rotea, R., Martínez, V., 2016. Roman military settlements in the Northwest of the Iberian Peninsula. The contribution of historical and modern aerial photography, satellite imagery and airborne LiDAR. AARGnews 52, 43–51.

Crutchley, S., 2006. Light detection and ranging (lidar) in the Witham Valley, Lincolnshire: an assessment of new remote sensing techniques. Archaeol. Prospect. 13, 251–257. https://doi.org/10.1002/arp.294.

Danese, M., Gioia, D., Vitale, V., Abate, N., Amodio, A.M., Lasaponara, R., Masini, N., 2022. Pattern recognition approach and LiDAR for the analysis and mapping of archaeological looting: application to an Etruscan site. Remote Sens. (Basel) 14, 1587. https://doi.org/10.3390/rs14071587.

Davis, L., Annan, A.P., 1989. Ground penetrating radar for high-resolution mapping of soil and rock stratigraphy. Geophys. Prospect. 37, 531–551.

Davis, D.S., Sanger, M.C., Lipo, C.P., 2019. Automated mound detection using lidar and object-based image analysis in Beaufort County, South Carolina. Southeast. Archaeol. 38, 23–37. https://doi.org/10.1080/0734578X.2018.1482186.

De Smedt, P., Saey, T., Lehouck, A., Stichelbaut, B., Meerschman, E., Islam, M.M., Van De Vijver, E., Meirvenne, M., 2013. Exploring the potential of multi-receiver EMI survey for geoarchaeological prospection: A 90 ha dataset. Geoderma 40, 1260–1267.

Deiana, R., Vicenzutto, D., Deidda, G.P., Boaga, J., Cupitò, M., 2020. Remote sensing, archaeological, and geophysical data to study the terramare settlements: The case study of Fondo Paviani (Northern Italy). Remote Sens. (Basel) 12 (16), 2617. https://doi.org/10.3390/rs12162617.

Deiana, R., Deidda, G.P., Cusí, E.D., van Dommelen, P., Stiglitz, A., 2022. FDEM and ERT measurements for archaeological prospections at Nuraghe S'Urachi (West-Central Sardinia). Archaeol. Prospect. 29 (1), 69–86. https://doi.org/10.1002/arp.1838.

Delefortrie, S., Hanssens, D., De Smedt, P., 2018. Low signal-to-noise FDEM in-phase data: Practical potential for magnetic susceptibility modelling. J. Appl. Geophys. 152, 17–25. https://doi.org/10.1016/j.jappgeo.2018.03.003.

Di Maio, R., Meola, C., Grimaldi, M., Pappalardo, U., 2012. New insights for conservation of Villa Imperiale (Pompeii, Italy) through non-destructive exploration. Int. J. Architectural Heritage 6 (5), 562–578. https://doi.org/10.1080/15583058.2011.593392.

Di Maio, R., La Manna, M., Piegari, E., 2016. 3D reconstruction of buried structures from magnetic, electromagnetic and ERT data: Example from the archaeological site of Phaistos (Crete, Greece). Archaeol. Prospect. 23, 287–299.

Di Maio, R., La Manna, M., Piegari, E., Zara, A., Bonetto, J., 2018. Reconstruction of a Mediterranean coast archaeological site by integration of geophysical and archaeological data: the Nora town (Cagliari, Italy). J. Archaeol. Sci. Rep. 20, 230–238. https://doi.org/10.1016/j.jasrep.2018.05.003.

Doneus, M., 2013. Openness as Visualization Technique for Interpretative Mapping of Airborne Lidar Derived Digital Terrain Models. Remote Sens. 5, 6427–6442. https://doi.org/10.3390/rs5126427.

Drahor, M.G., Göktürkler, G., Berge, M.A., Kurtulmus, T.Ö., Tuna, N., 2007. 3D resistivity imaging from an archaeological site in south-western Anatolia, Turkey: a case study. Near Surf. Geophys. 5, 195–201.

Esposito, L., 2010. Le Pergamene dell'Archivio vescovile di Caiazzo (1286–1309). Arte Tipografica, Napoli (Italy), p. 322.

Evans, D.H., Fletcher, R.J., Pottier, C., Chevance, J.-B., Soutif, D., Tan, B.S., Im, S., Ea, D., Tin, T., Kim, S., Cromarty, C., De Greef, S., Hanus, K., Baty, P., Kuszinger, R., Shimoda, I., Boornazian, G., 2013. Uncovering archaeological landscapes at Angkor using lidar. Proc. Natl. Acad. Sci. 110, 12595–12600. https://doi.org/10.1073/pnas.1306539110.

Fassbinder, J.W.E., 2015. Seeing beneath the farmland, steppe and desert soil: magnetic prospecting and soil magnetism. J. Archaeol. Sci. 56, 85–95.

Fassbinder, J.W.E., 2017. Magnetometry for Archaeology. In Gilbert A.S. (Ed.): *Encyclopedia of Geoarchaeology*. Encyclopedia of Earth Sciences Series. Springer, Dordrecht. https://doi.org/10.1007/978-1-4020-4409-0_169.

Fiorillo, R., 2012. Sistemi insediativi a confronto nella Campania altomedioevale. La pianura pestana, In Galetti P. (Ed.): *Paesaggi, comunità, villaggi medievali*, Fondazione CISAM (Centro Italiano di Studi sull'Alto Medioevo), Spoleto (Italy), 723-727, ISBN: 9788879883474.

Frisetti, A., 2019. Paesaggi e insediamenti medievali in una vivace area di confine: la media valle del Volturno, in Medioevo nelle valli. In F. Marazzi, C. Raimondo (Eds.): *Insediamento, società, economia nei comprensori di valle tra Alpi e Appennini (VIII-XIV sec.)*, Volturnia Edizioni, Cerro a Volturno (Isernia, Italy), 333-348, ISBN 978-88-96092-99-6.

Gaffney, C., 2008. Detecting trends in the prediction of buried past: a review of geophysical techniques in archaeology. Archaeometry 50 (2), 313–336.

Gattula, E., 1733. Historia Abbatiae Cassinensis. Venezia (Italy).

Gattula, E., 1734. Accessiones ad Historiam Abbatiae Casinensis, Venezia (Italy).

Giannetti, A., 1973. Epigrafi latine della Campania e del Latium Adiectum. Rendiconti dell'Accademia Nazionale dei Lincei 28, 469–495.

Grinc, M., 2015. 3D GPR investigation of pavement using 1 GHz and 2 GHz horn type antenna - Comparison of the results. Contrib. Geophys. Geodesy 45 (1), 25–39.

Guyot, A., Lennon, M., Hubert-Moy, L., 2021. Objective comparison of relief visualization techniques with deep CNN for archaeology. J. Archaeol. Sci. Rep. 38, 103027.

Henry, E.R., Wright, A.P., Sherwood, S.C., Carmody, S.B., Barrier, C.R., Van de Ven, C., 2020. Beyond never-never land: Integrating LiDAR and geophysical surveys at the Johnston Site, Pinson Mounds State Archaeological Park, Tennessee, USA. Remote Sens. (Basel) 12 (15), 2364. https://doi.org/10.3390/rs12152364.

Horňák, M., Zachar, M., 2017. Some Examples of Good Practice in LiDAR Prospection in Preventive Archaeology. Interdisciplinaria Archaeologica - Natral Sciences in Archaeology, VIII 113–124. https://doi.org/10.24916/iansa.2017.2.1.

Khan, S., Aragão, L., Iriarte, J., 2017. A UAV-lidar system to map Amazonian rainforest and its ancient landscape transformations. Int. J. Remote Sens. 38, 2313–2330. https://doi.org/10.1080/01431161.2017.1295486.

Kokalj, Ž., Zakšek, K., Oštir, K., Pehani, P., Čotar, K., Somrak, M., 2019. Relief Visualization Toolbox, ver. 2.0 Manual, https://www.zrc-sazu.si/sites/default/files/rvt_2.2.1_0.pdf.

Kokalj, Ž., Hesse, R., 2017. Airborne laser scanning raster data visualization. A Guide to Good Practice. Prostor, kraj, čas 14. https://doi.org/10.3986/9789612549848.

Křivánek, R., 2017. Comparison study to the use of geophysical methods at archaeological sites observed by various remote sensing techniques in the Czech Republic. Geosciences 7 (3), 81. https://doi.org/10.3390/geosciences7030081.

Lambers, K., 2018. Airborne and Spaceborne Remote Sensing and Digital Image Analysis in Archaeology. In: Siart, C., Forbriger, M., Bubenzer, O. (Eds.), Digital GeoArchaeology: New Techniques for interdisciplinary Human-Environmental Research, Natural Science in Archaeology. Springer International Publishing, Cham, pp. 109–122. https://doi.org/10.1007/978-3-319-25316-9_7.

Leckebusch, J., 2000. Two- and three-dimensional georadar surveys across a medieval choir: A case study in archaeology. Archaeol. Prospect. 7 (3), 189–200.

Leucci, G., De Giorgi, L., Di Giacomo, G., Ditaranto, I., Miccoli, I., Scardozzi, G., 2016. 3D GPR survey for the archaeological characterization of the ancient Messapian necropolis in Lecce, South Italy. J. Archaeol. Sci.: Reports 7, 290–302.

Loré, V., 2012. I villaggi nell'Italia meridionale (secoli IX-XI): problemi di definizione. In Galetti P. (Ed.): *Paesaggi, comunità, villaggi medievali*, Fondazione CISAM (Centro Italiano di Studi sull'Alto Medioevo), Spoleto (Italy), 535-546, ISBN: 9788879883474.

Lozić, E., Štular, B., 2021. Documentation of Archaeology-Specific Workflow for Airborne LiDAR Data Processing. Geosciences 11, 26. https://doi.org/10.3390/geosciences11010026.

Luo, L., Wang, X., Guo, H., Lasaponara, R., Zong, X., Masini, N., Wang, G., Shi, P., Khatteli, H., Chen, F., Tariq, S., Shao, J., Bachagha, N., Yang, R., Yao, Y., 2019. Airborne and spaceborne remote sensing for archaeological and cultural heritage applications: A review of the century (1907–2017). Remote Sens. Environ. 232, 111280 https://doi.org/10.1016/j.rse.2019.111280.

Marazzi, F., 2011. San Vincenzo al Volturno dal X al XII secolo. Le "molte vite" di un monastero fra poteri universali e trasformazioni geopolitiche del Mezzogiorno. In: *Fonti per la storia dell'Italia Medievale*, Subsidia, 10, Roma (Italy): Istituto Storico Italiano per il Medio Evo, 1-252, ISBN: 978-88-89190-78-4.

Marazzi, F., 2016. Pellegrini e fondatori. Rapporti fra monasteri e politica nel Meridione altomedioevale. In: *Bullettino dell'Istituto Storico per il Medio Evo*, 118, 49-108, ISSN: 1127-6096.

Masini, N., Coluzzi, R., Lasaponar, R., 2011. On the Airborne Lidar Contribution in Archaeology: from Site Identification to Landscape Investigation. In: Wang, C.-C. (Ed.), *Laser Scanning, Theory and Applications*. InTech. https://www.intechopen.com/chapters/15810.

Masini, N., Gizzi, F., Biscione, M., Fundone, V., Sedile, M., Sileo, M., Pecci, A., Lacovara, B., Lasaponara, R., 2018. Medieval Archaeology Under the Canopy with LiDAR. The (Re)Discovery of a Medieval Fortified Settlement in Southern Italy. Remote Sens., 10, 1598, https://doi.org/10.3390/rs10101598.

McNeill, J.D., 1980. Electromagnetic terrain conductivity measurement at low induction numbers. Technical Note TN-6. Geonics Ltd., Mississauga, ON.

Merola, R., 2007. Un insediamento della terra S. Benedicti. Il castrum di San Pietro in Flia tra X e XIII secolo. In: *Quaderni Campano-Sannitici*, IX, Piedimonte Matese, p.18.

Miller, B.V., Payne, J.D., Killion III, W.F., Adams, R.F., 2019. Geophysical surveys and geospatial data for Bob Kidd Lake, Washington County, Arkansas: U.S. Geological Survey data release, https://doi.org/10.5066/P9I4W2P0.

Mommsen T., 1883. *Corpus inscriptionum latinarum. Inscriptiones Calabriae, Apuliae, Samnii, Sabinorum, Piceni Latinae,* I-XVII, TH. Mommsen (Ed.), Berolini, 477 pp.

Pavoni, M., Sirch, F., Boaga, J., 2021. Electrical and electromagnetic geophysical prospecting for the monitoring of rock glaciers in the Dolomites, Northeast Italy. Sensors, 21, 1294, https://doi.org/10.3390/s21041294.

Peduto, P., 1984. Villaggi fluviali nella pianura pestana del Secolo VII. La chiesa e la necropoli di S. Lorenzo di Altavilla Silentina. Edizioni Studi Storici Meridionali, Salerno (Italy), 306 pp.

Pueyo Anchuela, Ó., Diarte Blasco, P., García Benito, C., Casas Sainz, A.M., Pocoví, J.A., 2016. Geophysical and archaeological characterization of a modest roman villa: methodological considerations about progressive feedback analyses in sites with low geophysical contrast. Archaeol. Prospect. 23 (2), 105–123. https://doi.org/10.1002/arp.1529.

Reynolds, J.M., 2011. An Introduction to Applied and Environmental Geophysics, second edition. John Wiley & Sons, Chichester, p. 712.

Richards-Rissetto, H., Newton, D., Al Zadjali, A., 2021. A 3D point cloud deep learning approach using lidar to identify ancient Maya archaeological sites. ISPRS Ann. Photogramm. Remote Sens. Spat. Inf. Sci. VIII-M-1-2021, 133–139. https://isprs-annals.copernicus.org/articles/VIII-M-1-2021/133/2021/.

Saey, T., De Smedt, P., Monirul, I.M., Meerschman, E., Van De Vijver, E., Lehouck, A., Van Meirvenne, M., 2012. Depth slicing of multi-receiver EMI measurements to enhance the delineation of contrasting subsoil features. Geoderma 189–190, 514–521.

Saey, T., Van Meirvenne, M., De Smedt, P., Stichelbaut, B., Delefortrie, S., Baldwin, E., Gaffney, V., 2015. Combining EMI and GPR for non-invasive soil sensing at the Stonehenge World Heritage Site: The reconstruction of a WW1 practice trench. Eur. J. Soil Sci. 66, 166–178.

Scollar, I., Tabbagh, A., Hesse, A., Herzog, I., 2009. Archaeological prospecting and remote sensing. Cambridge University Press, Cambridge, p. 696.

Scudero, S., Martorana, R., Capizzi, P., Pisciotta, A., D'Alessandro, A., Bottari, C., Di Stefano, G., 2018. Integrated geophysical investigations at the Greek Kamarina site (Southern Sicily, Italy). Surv. Geophys. 39 (6), 1181–1200.

Silliman, S.W., Farnsworth, P., Lightfoot, K.G., 2000. Magnetometer prospecting in historical archaeology: evaluating survey options at a 19th-century rancho site in California. Hist. Archaeol. 34 (2), 89–109.

Staffa, A.R., 2006. Paesaggi ed insediamenti rurali dell'Abruzzo adriatico fra tardo antico e Altomedioevo. In: Volpe, G., Turchiano, M. (Eds.), Paesaggi e insediamenti rurali nell'Italia meridionale. Edipuglia, Bari (Italy), pp. 39–125.

Štular, B., Lozić, E., 2020. Comparison of Filters for Archaeology-Specific Ground Extraction from Airborne LiDAR Point Clouds. Remote Sens. (Basel) 12, 3025. https://doi.org/10.3390/rs12183025.

Štular, B., Weichert, S., Lozić, E., 2021a. Airborne LiDAR Point Cloud Processing for Archaeology. Pipeline and QGIS Toolbox. Remote Sensing 13, 3225. https://doi.org/10.3390/rs13163225.

Štular, B., Lozić, E., Eichert, S., 2021b. Airborne LiDAR-Derived Digital Elevation Model for Archaeology. Remote Sens. (Basel) 13, 1855. https://doi.org/10.3390/rs13091855.

Štular, B., Lozić, E., Eichert, S., 2023. Interpolation of airborne LiDAR data for archaeology. J. Archaeol. Sci. Rep. 48 https://doi.org/10.1016/j.jasrep.2023.103840.

Wolff, C.B., Urban, T.M., 2013. Geophysical analysis at the Old Whaling site, Cape Krusenstern, Alaska, reveals the possible impact of permafrost loss on archaeological interpretation. Polar Res. 32 (1), 19888. https://doi.org/10.3402/polar.v32i0.19888.

Won, I.J., Huang, H., 2004. Magnetometers and electromagnetometers. Lead. Edge 23, 448–451.

Yilmaz, O., 1987. Seismic Data Processing. Society of Exploration Geophysicists, Tulsa OK, p. 526.

Yilmaz, S., Balkaya, Ç., Çakmak, O., Oksum, E., 2019. GPR and ERT explorations at the archaeological site of Kılıç village (Isparta, SW Turkey). J. Appl. Geophys. 170, 103859.

Zambardi, M., 2009a. Rinvenimenti archeologici nel sito di Ad Flexum. In: Per la conoscenza dei beni culturali II. Seconda Università degli Studi di Napoli, Napoli, pp. 41–51.

Zambardi, M., 2007a. La via Latina nel territorio di Ad Flexum. In: *Ager Aquinas. Storia e archeologia nella media valle dell'antico Liris II.* Spigolature Aquinati. Giornata di studio-Aquino, 19 maggio 2007, A. Nicosia, G. Ceraudo (Eds.), 121-132.

Zambardi, M., 2007b. Organizzazione del territorio in corrispondenza della mansio "Ad Flexum". In: *Casinum Oppidum*, Atti della Giornata di Studi su Cassino preromana e romana (Cassino, Biblioteca Comunale 8 ottobre 2004), Cassino, 161-169.

Zambardi, M., 2009b. San Pietro Infine: il sito di Ad Flexum. Bollettino trimestrale di studi storici del Lazio meridionale, 9(2), 92-95.